Atherosclerosis 244 (2016) 101–107

Contents lists available at ScienceDirect

Atherosclerosis

journal homepage: www.elsevier.com/locate/atherosclerosis

Early *in vivo* discrimination of vulnerable atherosclerotic plaques that disrupt: A serial MRI study

Tuan A. Pham [b], Ning Hua [a], Alkystis Phinikaridou [c], Ronald Killiany [d], James Hamilton [a, b, *]

[a] Department of Physiology and Biophysics, Boston University School of Medicine, Boston, MA, USA
[b] Department of Biomedical Engineering, Boston University, Boston, MA, USA
[c] Division of Imaging Sciences and Biomedical Engineering, King's College London, London, United Kingdom
[d] Department of Anatomy and Neurobiology, Boston University School of Medicine, Boston, MA, USA

ARTICLE INFO

Article history:
Received 31 August 2015
Received in revised form
8 November 2015
Accepted 10 November 2015
Available online 14 November 2015

Keywords:
Atherosclerosis
Remodeling
MRI
Plaque rupture
Plaque progression

ABSTRACT

Background and aims: MRI has been validated as a suitable imaging modality for *in vivo*, non-invasive detection of atherosclerosis and has provided quantitative predictors of high-risk plaque. Here, we apply serial MRI to monitor the natural progression of plaques over a 3-month period in a rabbit model of atherothrombosis to determine differences over time between plaques that ultimately disrupt to form a luminal mural thrombus and plaques that remain stable.

Methods: Atherosclerotic plaques were induced in 12 male New Zealand White (NZW) rabbits by aortic endothelial injury and a 1% cholesterol diet. The rabbits were imaged 5 times: at baseline, 1, 2, and 3 months, and 48hr after pharmacological triggering for plaque disruption.

Results: Starting at 2 months, plaques that disrupted after triggering exhibited a higher remodeling ratio (RR, 1.05 ± 0.11 vs 0.97 ± 0.10, $p = 0.0002$) and a larger vessel wall area (VWA, 6.99 ± 1.54 mm^2 vs 6.30 ± 1.37 mm^2, $p = 0.0072$) than the stable non-disrupted plaques. The same trends were observed at 3 months: plaques that disrupted had a higher RR (1.04 ± 0.02 vs 0.99 ± 0.01, $p = 0.0209$), VWA (8.19 ± 2.69 mm^2 vs 6.81 ± 1.60 mm^2, $p = 0.0001$), and increased gadolinium uptake (75.51 ± 13.77% for disrupted vs 31.02 ± 6.45% for non-disrupted, $p = 0.0022$).

Conclusions: MR images of plaques that disrupted revealed larger VWAs, RRs, and increased gadolinium uptake at 2 months and continued progression of these vulnerable features between 2 and 3 months. Non-disrupted plaques had an independent history without these hallmarks of vulnerability. Our results show that MRI can provide early detection of plaques at a higher-risk for luminal thrombosis.

1. Background

Atherosclerotic plaque rupture or erosion and subsequent luminal/mural thrombus formation [1] may lead to myocardial infarction and stroke [2,3], which are major causes of death in the United States [4]. The ability to noninvasively monitor changes in atherosclerotic lesion features *in vivo* could provide insights into the development of plaque vulnerability and identification of plaques that are at high-risk for thrombosis [5]. Studies of the natural evolution of plaques in humans have many limitations, including the long duration of plaque progression and the inability to induce disruption as an endpoint for determining the high-risk plaques or to follow a specific plaque from an early stage to its disruption. Thus, studies of animal models with validated histology and *in vivo* characteristics that replicate human disease are invaluable for providing insights into human plaque progression and regression.

Magnetic Resonance Imaging (MRI) has been shown to be a valuable imaging modality of atherosclerotic lesions in both humans and animal models [6–11]. It has been used to visualize and quantify changes in atherosclerotic plaques over time in both small (mouse [8,12,13]) and large (rabbits [14–16], pigs [17,18]) animals. Mouse plaques differ from human plaques, limiting their relevance to human disease [19,20]. Even with these limitations, *in vivo* MRI of mice models have provided information on luminal narrowing, vascular remodeling [12], and other characteristics of

* Corresponding author. Department of Physiology and Biophysics, Boston University School of Medicine, 700 Albany Street, W302, Boston, MA 02118-2526, USA.
E-mail address: jhamilt@bu.edu (J. Hamilton).

http://dx.doi.org/10.1016/j.atherosclerosis.2015.11.013
0021-9150/

atherosclerosis [8,12,13]. MRI studies in pig carotid arteries have provided information on disease states and vulnerability [18]. Studies of pig coronary arteries have shown features similar to those in our rabbit model in plaques that disrupt [21]. Although pig models have been reported to exhibit plaque rupture with distal embolism [22], there is a lack of reports of controlled thrombosis with attached luminal thrombus in pigs.

Because rabbit models can generate plaques that have luminal disruption as well as plaques that exhibit similarities to human coronary and carotid plaques [25], studies of rabbit models are potentially more translatable to the clinical setting. An early MRI study at 1.5T on NZW rabbits fed a low (0.2%) cholesterol diet for an extended period (14–16 months) with two balloon injuries in the abdominal aorta visualized changes in plaque features between 9 and 16 months [14]. NZW rabbits fed 0.3% cholesterol without balloon injury did not show significant outward remodeling even at 20 months [23]. In another study without balloon injury, NZW rabbits with cholesterol feeding (0.3%) for 4 months were imaged at 4, 12, and 20 months later to compare progression and regression [7]. In contrast, a Watanabe model with aortic balloon injury showed compensatory remodeling with MRI [15]. However, these studies define vulnerability based on histological plaque characteristics, rather than plaque disruption [1] and the different protocols for inducing atherosclerosis make cross study comparisons of results difficult.

The novelty of the work presented here is the application of serial MRI to monitor the evolution of plaques that ultimately disrupt following pharmacological triggering. Our modified Constantinides rabbit model [24,25] of atherothrombosis exhibits complex lesions encompassing 6 of the 8 American Heart Association (AHA) established human plaque classifications [26,27] and replicates many histological [26] and imaging [9,28] features of disrupted human plaques. Here, we apply MRI measurements previously made only at the end of protocol to monitor development and differentiation of individual plaques over our 3 month our preparation period.

2. Methods

2.1. Rabbit model of atherosclerosis

The rabbit model used was prepared as previously described [9,26]. Briefly, male NZW rabbits (n = 12, 2.8–3 kg) were purchased (Pine Acres, Norton, MA) and atherosclerotic lesions were induced with a high fat diet (HFD) in conjunction with aortic wall denudation via balloon catheter under general anesthesia (acepromazine, 0.75 mg/kg IM; ketamine, 35 mg/kg IM; xylazine, 2.5 mg/kg IM). Plaque disruption was triggered twice, within 48 h, using Russell Viper Venom (RVV, 0.15 mg/kg IP; Enzyme Research, South Bend, IN), followed 30 min later by histamine (0.02 mg/kg IV; Sigma–Aldrich, St. Louis, Mo) as presented in Fig. 1. See supplemental materials for more details.

Of the twelve rabbits, one became unhealthy and did not complete the study due to suspected multi-organ dysfunction. All animal studies were performed in strict adherence to guidelines approved by the Institutional Animal Care and Use Committee of Boston University.

2.2. Serial MRI

Rabbits were imaged a total of 5 times with identical scanning procedures (Fig. 1) in a 3.0-T Philips Intera Scanner (Philips Medical Systems, Ohio) as previously described in detail [9]. Un-gated coronal 3D phase contrast MR angiograms (PC-MRA) were obtained to visualize the vasculature and fat suppressed, T1-weighted black blood (T1BB-FS) axial images were obtained with ECG gating in 4 mm increments to visualize the vessel wall. Another set of T1BB-FS images with the exact same parameters was taken 15 min after gadolinium-diethylenetriamine penta-acetic acid (Gd-DTPA) injection (0.1 mmol/kg IV) (Magnevist, Germany). See supplemental materials for more detail.

2.3. Identifying vulnerable plaques and matching scan data

Disrupted plaques were defined as those with a mural thrombus present in the post-trigger MR images and non-disrupted plaque as those that lacked thrombus [9]. To align corresponding MRI images between serial scans, the distances from the iliac bifurcation and left renal artery were used as internal anatomical landmarks. Previous work showed that the MRI methods used here were able to accurately detect plaque disruption and subsequent thrombus formation, as proved by histology [9].

2.4. Image analysis

To follow a specific plaque over a time series of MRI scans, plaque segments were aligned as above to match corresponding images from different scans. Of the 212 plaque segments visualized using T1BB-FS images, a total of 181 segments were analyzed and the remaining segments (14.6%) were excluded due to poor image quality. For each plaque segment, both the T1BB-FS and the CET1BB-FS images were manually segmented using ImageJ (NIH) for 1, 2 and 3 month (pre-trigger) scans. The post-trigger images were only used to categorize each plaque segment as non-disrupted (no thrombus, Fig. 2A Non-disrupted) or disrupted (attached thrombus, Fig. 2A Disrupted, red arrow).

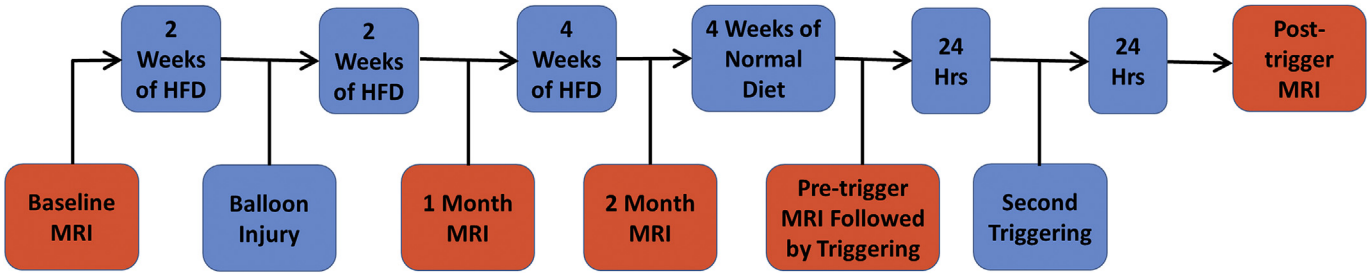

Fig. 1. Timeline of rabbit atherosclerosis protocol and imaging session schedule. The rabbits are fed a 1% high cholesterol diet for a total of 2 months, with an aortic inundation balloon catheter surgery performed 2 weeks into the feeding protocol. Then, 4 week period of normal rabbit chow occurs prior to plaque trigger. MRIs taken at 0, 1, 2, 3 months, and 24hr after the second triggering.

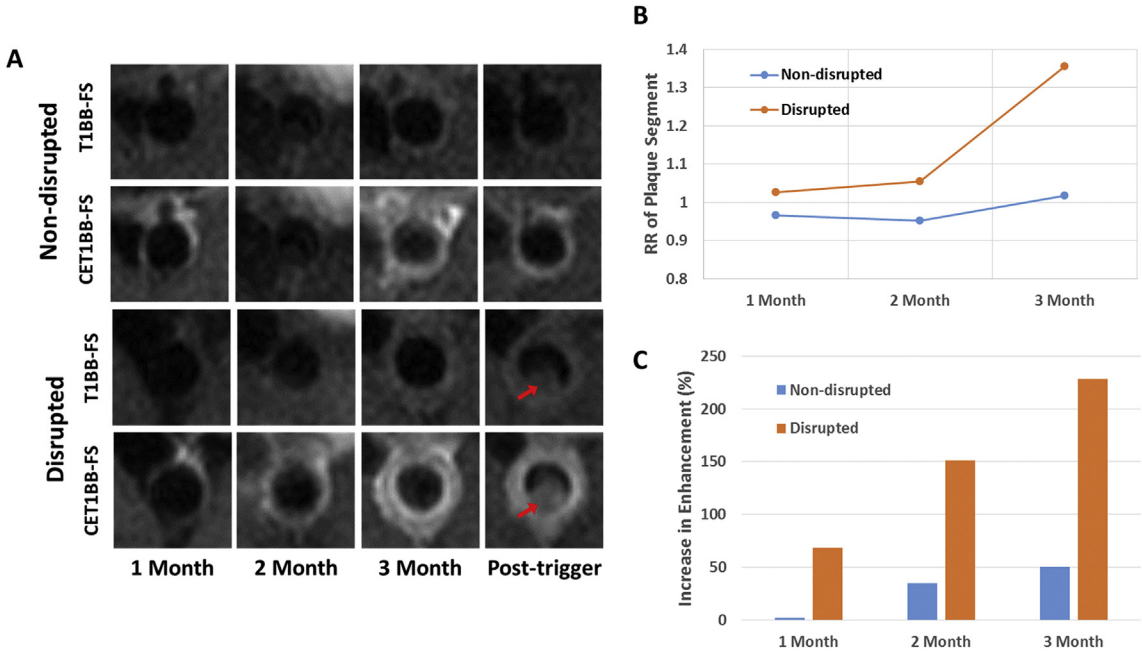

Fig. 2. A) Example of serial images of a disrupted and a non-disrupted plaque in the same rabbit aorta. The red arrow points to a luminal thrombus. B) Remodeling Ratio (RR) of plaque segments shown in A, which shows an increasing RR value for the disrupted plaque and a stable RR value for the non-disrupted plaque. C) Increase in contrast enhancement of the plaques shown in A. The disrupted plaque showed a much greater increase in signal enhancement over time than the non-disrupted plaque. (For interpretation of the references to colour in this figure legend, the reader is referred to the web version of this article.)

T1BB-FS images were used to calculate the vessel area (VA) and the lumen area (LA), the vessel wall area (VWA = VA − LA) and the remodeling ratio (RR). The RR was calculated after correcting for arterial tapering and individual differences between rabbits [9,29]. Briefly, the RR is the ratio of the outer vessel wall area of a plaque segment with respect to the outer vessel wall area of a reference segment. The segment chosen for the reference has the smallest VWA (assumed to be least affected by atherosclerosis). A plaque segment is classified has having negative remodeling (RR < 0.95), intermediate remodeling (0.95 ≤ RR ≤ 1.05), or positive remodeling (RR > 1.05) based on the value of RR [29]. These calculations were done for each rabbit at each time point.

To assess gadolinium uptake, the CET1BB-FS images were manually segmented and normalized to an external standard. The average VWA signal intensity obtained at baseline was used to normalize the values obtained for all the subsequent scanning sessions and the results were expressed as a % increase from baseline of the signal intensity as shown below:

$$\frac{CE_{plaque}}{CE_{baseline}} \times 100 - 100 = \%\ Increase\ from\ Baseline$$

Where CE_{plaque} is the normalized signal intensity of the plaque segment at the analyzed time point and $CE_{baseline}$ is the normalized signal intensity of the same plaque segment at baseline.

2.5. Statistical analysis

All statistical analysis was performed using Excel (Microsoft, Redmond WA). For comparisons between disrupted and non-disrupted plaques, a Student's t-test was used to determine if the two samples had different means. Data are presented as mean ± standard error in figures, tables and text. Probability values of $P < 0.05$ were considered significant.

3. Results

3.1. Serial MRI can differentiate at-risk and stable plaques over time

Atherosclerotic plaques were observed in 11 rabbits by MRI, 10 of which developed thrombus. A total of 181 plaque segments were analyzed, 39 (21.5%) of which were classified as disrupted. Fig. 2A shows example serial images of a disrupted and a non-disrupted plaque within the same rabbit. A qualitative assessment of the VWA and signal enhancement showed that the both plaques were similar at 1 month. At 2 months, the two types of plaques became different with respect to the RR and contrast enhancement. The non-disrupted plaque showed a small increase in RR and signal enhancement, while the disrupted plaque showed a significant increase in RR and signal enhancement. The quantitative changes for these two specific plaques are plotted in Fig. 2B and C.

On average, both plaque types exhibited no significant differences in all parameters measured at 1 month, but began to show differences at 2 months (Figs. 3 and 4). Disrupted plaques had larger VWA (Fig. 3) compared to non-disrupted plaques at 2 and 3 months (6.99 ± 0.25 mm^2 vs 6.30 ± 0.11 mm^2; $p = 0.0072$ and 8.19 ± 0.43 mm^2 vs 6.81 ± 0.13; $p = 0.0001$, respectively). The RR of the disrupted and non-disrupted plaques followed a similar pattern (1.05 ± 0.02 vs 0.97 ± 0.01; $p = 0.0002$ at 2 months and 1.04 ± 0.02 vs 0.99 ± 0.01; $p = 0.0209$ at 3 months). The findings at 3 months agree with our previous findings [9] and both measurements have been associated with plaque vulnerability in numerous studies [9,30–33].

Disrupted plaques also shifted towards higher RR values (Fig. 4) as the disease progressed, while non-disrupted plaques had an RR value distribution that was relatively stable over time. The disrupted plaques started with ~31% of the plaques having an RR > 1.05, which increased to over 40% of the plaques having an RR > 1.05 by the last time point. Only 24% of the non-disrupted plaques had a RR > 1.05 at 1 month and the distribution

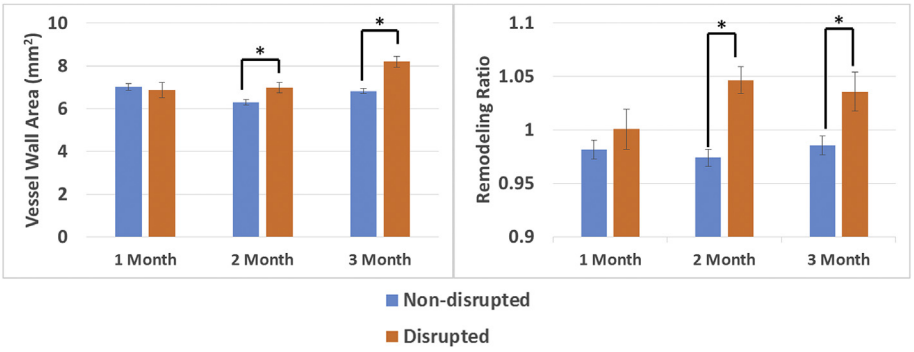

Fig. 3. Vessel wall area (VWA) and remodeling ratio (RR) over time. The VWA and RR both showed statistically significant differences between disrupted and non-disrupted plaques starting at 2 months.

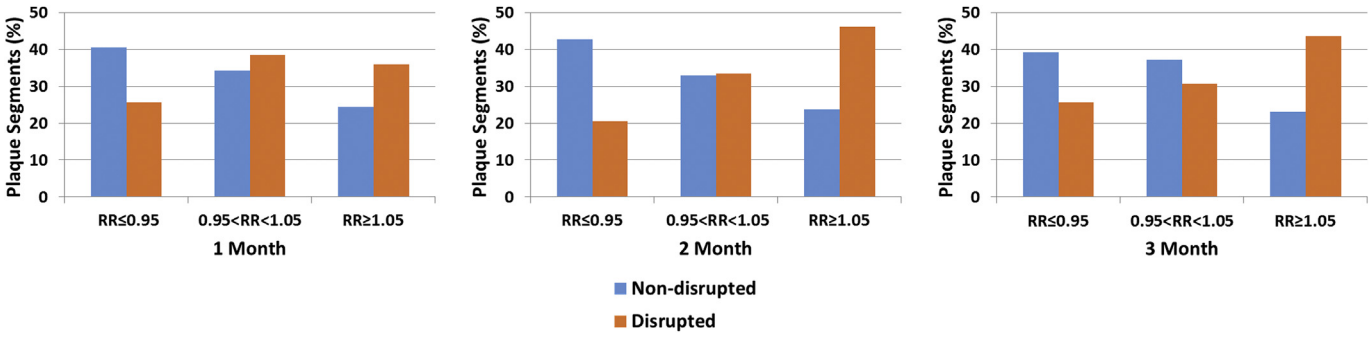

Fig. 4. Progression of remodeling ratio (RR) distributions between non-disrupted and disrupted plaques. Over disease development, the disrupted plaques exhibited higher RR values, while non-disrupted plaques showed very little shift in RR.

remained nearly unchanged by the end of the experiment.

Fig. 5 shows that there is a general increase in the uptake of the contrast agent Gd-DTPA during atherosclerosis progression. Differences in the % increase of signal intensity between disrupted and non-disrupted plaques were seen at each month, but became significant at 3 months (75.51 ± 13.77% for disrupted vs 31.02 ± 6.45% for non-disrupted, $p = 0.0022$).

The averaged numerical values for measurements of VWA, remolding ratio, and gadolinium enhancement for each MRI scan are presented Tables 1, 2 and 3 (supplemental materials).

4. Discussion

This serial MRI study, monitoring the natural progression of atherosclerotic plaques, revealed some remarkable examples of independent development of plaques within the same aorta. Our results showed that on average VWA, RR and gadolinium uptake were different in stable and disrupted plaques at both 2 and 3 months. All three became more pronounced at month 3, even after the rabbits were switched to normal chow.

Most characteristics of vulnerable plaques have been gleaned from morphological studies, but with greater interest in clinical applications, there has been a much needed shift from morphological attributes, to specific cardiac events as end points. Despite the many advances in the understanding of specific morphological and biological features, a compelling argument can be made for relevant translational animal models that produce vulnerable plaques at risk for rupture [1]. The fact that the majority of human

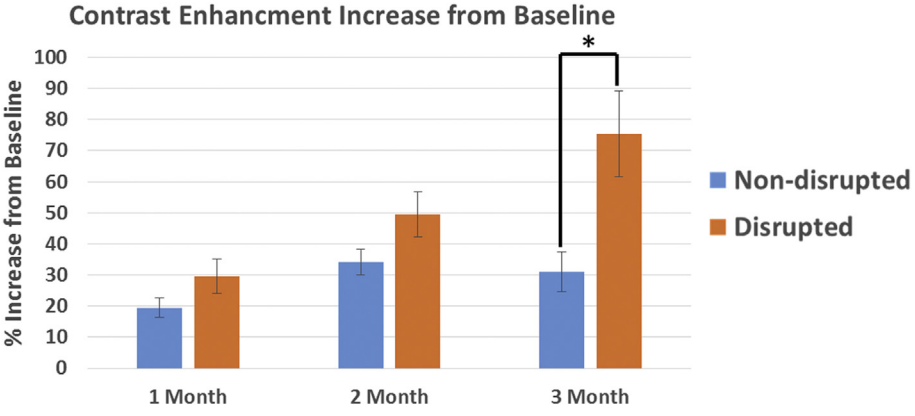

Fig. 5. Contrast enhancement increase over baseline for disrupted and non-disrupted segments. Disrupted plaques showed a greater increase in enhancement.

plaques with vulnerable features do not disrupt, and very long prospective studies are required to validate the *in vivo* characteristics of the highest risk plaques, accentuates the value of an animal model with plaque disruption.

Our rabbit model provides not only an endpoint of disruption but also advantages of observing different plaques types in the same aorta at the end of the 3 month protocol when MR images are obtained. Our previous histology studies showed that increased vessel wall area, excessive outward remodeling, inflamed fibrous cap, adventitial breakdown and neovascularization were highly associated with plaques that disrupted [26]. Here, we applied our MRI diagnostic protocols to measure some hallmarks of high-risk plaques: VWA, RR and gadolinium uptake [9].

Our new data for RR quantified over time showed that at 1 month, the RRs of all plaques exhibited intermediate remodeling levels ($0.95 \leq RR \leq 1.05$). At 2 months, the non-disrupted plaques remained in the intermediate range, while the disrupted plaques increased into the positive remodeling category ($RR > 1.05$). Plaques that disrupted were more likely to progress to an outward remodeled state ($RR > 1.05$), while the plaques that did not disrupt had similar RR values between 1 and 3 months (Fig. 4). These results corroborate with our previous findings using MRI at only 3 months [9] and previous work using IVUS [21,31,34] and CT [30,35], which showed an association between positive remodeling and plaque vulnerability in animals and humans. This difference in RR between the two types of plaques could signify an important pathological change that triggers/transforms a plaque from stable, to a plaque at high-risk for disruption, which has been implicated in earlier studies without an endpoint of disruption [21]. Early positive RR and increased VWA suggest that plaque growth itself is a stimulating factor that triggers outward remodeling at sites of future vulnerability to avoid luminal narrowing [32,36,37]. This speculation is in agreement with the increased lipid content and inflammatory infiltrate seen in histological studies of positively remodeled rabbit plaques in our model [26]. Additionally, human studies have linked positive remodeling with increased macrophage content [33,38] and increased plaque volumes [38,39]. RR can potentially be used as an early marker of plaque vulnerability, thus helping clinicians select specific plaques to track as the disease progresses. Additionally, the RR could also be used as an efficacy marker for the testing of therapeutics.

Measurement of VWA is a common approach to detect and monitor plaque burden without high resolution of plaque components. In our study, VWA exhibited a larger increase for disrupted plaques compared to stable plaque starting at 2 months in both the individual example (Fig. 2) and the averaged data, in agreement with our previous work [9] and a characteristic of high-risk human lesions [30].

Uptake of Gd-DTPA was consistently higher in plaques that ultimately disrupt. In some specific examples (Fig. 2), the comparison of signal increase was very profound. Increased enhancement is likely caused by increased inflammation, neovascularization, and decreased vessel wall integrity over time as shown by our previous detailed histological work on rabbit plaques [26]. The patterns of gadolinium uptake in this study are complementary to results of other investigators showing increasing Gd-DTPA uptake as the atherosclerotic plaques progressed in both human [40,41] and rabbit models [42] compared with little or no gadolinium enhancement in healthy patients and control rabbits.

Inflammation is now recognized as a key pathology of all stages of atherosclerosis, but this finding shows that it may be a major driving force for thrombosis of plaques in the high-risk categories that can be measured by non-invasive MRI. Once inflammation starts, it can be a self-propagating process that continues even after lowering cholesterol intake and allow plaques advance to stages of higher risk. Our findings support conclusions of the pig model of coronary plaques that excessive remodeling is highly associated with plaque progression to higher vulnerability. The correspondence of higher gadolinium uptake with RR also supports the conclusion that the inflammation status of a plaque is a key factor in the evolution of plaques to the high-risk category [21]. The rabbit provides an excellent model for detecting high-risk plaque at an early stage and for systematic and controlled studies of therapeutics. Because the MRI measures features that are known to be characteristics of human plaques and our studies were performed on a clinical 3T scanner, they have the potential for clinical translation. Our MRI protocol could be used for early/intermediate stage detection of plaque disruption risk and lead to a new standard of care for diagnosing and monitoring of human atherosclerotic plaques, if confirmed in humans. The rabbit model used here cannot completely mimic atherosclerotic disease progression found in humans, but exhibits the complex plaques found in human plaques, and only plaques with multiple vulnerable features disrupt with our triggering mechanism [26]. Although the exact mechanism for plaque rupture in humans has not been identified, studies point toward platelet activation and adhesion [43,44], and the release of vasoconstriction molecules as possible critical steps in the process [45]. Using this as a basis, our model uses procoagulant factor (viper venom) and a vasoconstriction agent (histamine) as plaque rupture catalysts. The thrombus is in our rabbit is platelet-rich with fibrin and collagen [46], characteristics of thrombus formation in humans. Furthermore, balloon injury and cholesterol feeding in the rabbit has recently been shown to replicate features of human thrombosis including tissue factor expression and its regulation by NF-kappa B [47,48]. In spite of these limitations, the quantitative measurements by MRI as described in this study detect vulnerable plaque evolution prior to the triggering and predicts disruption in this model. For potential clinical translation, a limitation of this study is the time needed for manual segmentation of the MR images. However, some groups have reported the continuing development of automatic segmentation programs that show promise as a solution for this issue [49].

5. Conclusions

In this study, we showed that MRI can be used to visualize progressive atherosclerotic plaque development and discern plaque features associated with vulnerability to induced disruption (large VWA, positive remodeling, and increased gadolinium uptake) as early as 2 months in a rabbit model of atherosclerosis. These findings affirm the feasibility of using MRI as a tool for assessing and monitoring high-risk plaques, at least in pre-clinical animal models. The non-invasive nature of using MRI makes it possible to have longitudinal evaluation of the disease in animal models and offers a potential application for use in human studies of atherosclerosis. An unanswered clinical question is whether or not the reversal of vulnerable plaque features induces a reduction of plaque ruptures. This animal model can be used to gain further insights.

Appendix A. Supplementary data

Supplementary data related to this article can be found at http://dx.doi.org/10.1016/j.atherosclerosis.2015.11.013.

References

[1] A.V. Finn, M. Nakano, J. Narula, F.D. Kolodgie, R. Virmani, Concept of vulnerable/unstable plaque, Arterioscler. Thromb. Vasc. Biol. 30 (2010) 1282–1292.
[2] A.C. Vanderwal, A.E. Becker, C.M. Vanderloos, P.K. Das, Site of intimal rupture

or erosion of thrombosed coronary atherosclerotic plaques is characterized by an inflammatory process irrespective of the dominant plaque morphology, Circulation 89 (1994) 36–44.
[3] A. Farb, A.P. Burke, A.L. Tang, Y.H. Liang, P. Mannan, J. Smialek, R. Virmani, Coronary plaque erosion without rupture into a lipid core – a frequent cause of coronary thrombosis in sudden coronary death, Circulation 93 (1996) 1354–1363.
[4] D. Lloyd-Jones, R. Adams, M. Carnethon, G. De Simone, T.B. Ferguson, K. Flegal, E. Ford, K. Furie, A. Go, K. Greenlund, N. Haase, S. Hailpern, M. Ho, V. Howard, B. Kissela, S. Kittner, D. Lackland, L. Lisabeth, A. Marelli, M. McDermott, J. Meigs, D. Mozaffarian, G. Nichol, C. O'Donnell, V. Roger, W. Rosamond, R. Sacco, P. Sorlie, R. Stafford, J. Steinberger, T. Thom, S. Wasserthiel-Smoller, N. Wong, J. Wylie-Rosett, Y.L. Hong, W.G. MEMBERS, A.H.A.S. Comm, and S.S. Subcomm, Heart disease and stroke statistics-2009 update a report from the American heart association statistics committee and stroke statistics subcommittee, Circulation 119 (2009) 480–486.
[5] V. Aursulesei, Nature or the natural evolution of plaque: what matters? Maedica (Buchar) 8 (2013) 309–314.
[6] C. Yuan, K.W. Beach, L.H. Smith, T.S. Hatsukami, Measurement of atherosclerotic carotid plaque size in vivo using high resolution magnetic resonance imaging, Circulation 98 (1998) 2666–2671.
[7] M.V. McConnell, M. Aikawa, S.E. Maier, P. Ganz, P. Libby, R.T. Lee, MRI of rabbit atherosclerosis in response to dietary cholesterol lowering, Arterioscler. Thromb. Vasc. Biol. 19 (1999) 1956–1959.
[8] Z.A. Fayad, J.T. Fallon, M. Shinnar, S. Wehrli, H.M. Dansky, M. Poon, J.J. Badimon, S.A. Charlton, E.A. Fisher, J.L. Breslow, V. Fuster, Noninvasive in vivo high-resolution magnetic resonance imaging of atherosclerotic lesions in genetically engineered mice, Circulation 98 (1998) 1541–1547.
[9] A. Phinikaridou, F.L. Ruberg, K.J. Hallock, Y. Qiao, N. Hua, J. Viereck, J.A. Hamilton, In vivo detection of vulnerable atherosclerotic plaque by MRI in a rabbit model, Circ. Cardiovasc. Imaging 3 (2010), 323–U155.
[10] G. Helft, S.G. Worthley, V. Fuster, A.G. Zaman, C. Schechter, J.I. Osende, O.J. Rodriguez, Z.A. Fayad, J.T. Fallon, J.J. Badimon, Atherosclerotic aortic component quantification by noninvasive magnetic resonance imaging: an in vivo study in rabbits, J. Am. Coll. Cardiol. 37 (2001) 1149–1154.
[11] A. Millon, J.L. Mathevet, L. Boussel, P.L. Faries, Z.A. Fayad, P.C. Douek, P. Feugier, High-resolution magnetic resonance imaging of carotid atherosclerosis identifies vulnerable carotid plaques, J. Vasc. Surg. 57 (2013), 1046–U479.
[12] R.P. Choudhury, Z.A. Fayad, J.G. Aguinaldo, V.V. Itskovich, J.X. Rong, J.T. Fallon, E.A. Fisher, Serial, noninvasive, in vivo magnetic resonance microscopy detects the development of atherosclerosis in apolipoprotein E-deficient mice and its progression by arterial wall remodeling, J. Magn. Reson. Imaging 17 (2003) 184–189.
[13] M.R. Makowski, G. Varma, A.J. Wiethoff, A. Smith, K. Mattock, C.H. Jansen, A. Warley, M. Taupitz, T. Schaeffter, R.M. Botnar, Noninvasive assessment of atherosclerotic plaque progression in ApoE-/- mice using susceptibility gradient mapping, Circ. Cardiovasc. Imaging 4 (2011) 295–303.
[14] M.P. Skinner, C. Yuan, L. Mitsumori, C.E. Hayes, E.W. Raines, J.A. Nelson, R. Ross, Serial magnetic-resonance-imaging of experimental atherosclerosis detects lesion fine-structure, progression and complications in-vivo, Nat. Med. 1 (1995) 69–73.
[15] S.G. Worthley, G. Helft, V. Fuster, A.G. Zaman, Z.A. Fayad, J.T.T. Fallon, J.J. Badimon, Serial in vivo MRI documents arterial remodeling in experimental atherosclerosis, Circulation 101 (2000) 586–589.
[16] G. Helft, S.G. Worthley, V. Fuster, Z.A. Fayad, A.G. Zaman, R. Corti, J.T. Fallon, J.J. Badimon, Progression and regression of atherosclerotic lesions – monitoring with serial noninvasive magnetic resonance imaging, Circulation 105 (2002) 993–998.
[17] S.F. Pedersen, S.A. Thrysoe, W.P. Paaske, T. Thim, E. Falk, S. Ringgaard, W.Y. Kim, CMR assessment of endothelial damage and angiogenesis in porcine coronary arteries using gadofosveset, J. Cardiovasc. Magn. Reson. 13 (2011) 10.
[18] X.B. Jiang, W.S. Yuan, J.S. Wang, Z. Liu, D.H. Liu, Z.S. Shi, Matrix metalloproteinase-9 expression in carotid atherosclerotic plaque and contrast-enhanced MRI in a swine model, J. Neurointerv. Surg. 6 (2014) 24–28.
[19] P. Cullen, R. Baetta, S. Bellosta, F. Bernini, G. Chinetti, A. Cignarella, A. von Eckardstein, A. Exley, M. Goddard, M. Hofker, E. Hurt-Camejo, E. Kanters, P. Kovanen, S. Lorkowski, W. McPheat, M. Pentikainen, J. Rauterberg, A. Ritchie, B. Staels, B. Weitkamp, M. de Winther, M. Consortium, Rupture of the atherosclerotic plaque: does a good animal model exist? Arterioscler. Thromb. Vasc. Biol. 23 (2003) 535–542.
[20] F. Calara, M. Silvestre, F. Casanada, N. Yuan, C. Napoli, W. Palinski, Spontaneous plaque rupture and secondary thrombosis in apolipoprotein E-deficient and LDL receptor-deficient mice, J. Pathol. 195 (2001) 257–263.
[21] K.C. Koskinas, C.L. Feldman, Y.S. Chatzizisis, A.U. Coskun, M. Jonas, C. Maynard, A.B. Baker, M.I. Papafaklis, E.R. Edelman, P.H. Stone, Natural history of experimental coronary atherosclerosis and vascular remodeling in relation to endothelial shear stress: a serial, in vivo intravascular ultrasound study, Circulation 121 (2010) 2092–2101.
[22] Z.S. Shi, L. Feng, X. He, A. Ishii, J. Goldstine, H.V. Vinters, F. Vinuela, Vulnerable plaque in a Swine model of carotid atherosclerosis, AJNR Am. J. Neuroradiol. 30 (2009) 469–472.
[23] J.A. Ronald, R. Walcarius, J.F. Robinson, R.A. Hegele, B.K. Rutt, K.A. Rogers, MRI of early- and late-stage arterial remodeling in a low-level cholesterol-fed rabbit model of atherosclerosis, J. Magn. Reson. Imaging 26 (2007) 1010–1019.
[24] G.S. Abela, P.D. Picon, S.E. Friedl, O.C. Gebara, A. Miyamoto, M. Federman, G.H. Tofler, J.E. Muller, Triggering of plaque disruption and arterial thrombosis in an atherosclerotic rabbit model, Circulation 91 (1995) 776–784.
[25] P. Constantinides, R.N. Chakravarti, Rabbit arterial thrombosis production by systemic procedures, Arch. Pathol. 72 (1961) 197–208.
[26] A. Phinikaridou, K.J. Hallock, Y. Qiao, J.A. Hamilton, A robust rabbit model of human atherosclerosis and atherothrombosis, J. Lipid Res. 50 (2009) 787–797.
[27] H.C. Stary, Natural history and histological classification of atherosclerotic lesions: an update, Arterioscler. Thromb. Vasc. Biol. 20 (2000) 1177–1178.
[28] A. Phinikaridou, N. Hua, T. Pham, J.A. Hamilton, Regions of low endothelial shear stress colocalize with positive vascular remodeling and atherosclerotic plaque disruption: an in vivo magnetic resonance imaging study, Circ. Cardiovasc. Imaging 6 (2013) 302–310.
[29] G. Pasterkamp, C. Borst, E.J. Gussenhoven, W.P.T.M. Mali, M.J. Post, S.H.K. The, J.A. Reekers, F.G. Vandenberg, Remodeling of de-novo atherosclerotic lesions in femoral arteries – impact on mechanism of balloon angioplasty, J. Am. Coll. Cardiol. 26 (1995) 422–428.
[30] S. Motoyama, M. Sarai, H. Harigaya, H. Anno, K. Inoue, T. Hara, H. Naruse, J. Ishii, H. Hishida, N.D. Wong, R. Virmani, T. Kondo, Y. Ozaki, J. Narula, Computed tomographic angiography characteristics of atherosclerotic plaques subsequently resulting in acute coronary syndrome, J. Am. Coll. Cardiol. 54 (2009) 49–57.
[31] P. Schoenhagen, K.M. Ziada, S.R. Kapadia, T.D. Crowe, S.E. Nissen, E.M. Tuzcu, Extent and direction of arterial remodeling in stable versus unstable coronary syndromes – an intravascular ultrasound study, Circulation 101 (2000) 598–603.
[32] S. Glagov, E. Weisenberg, C.K. Zarins, R. Stankunavicius, G.J. Kolettis, Compensatory enlargement of human atherosclerotic coronary arteries, N. Engl. J. Med. 316 (1987) 1371–1375.
[33] A.M. Varnava, P.G. Mills, M.J. Davies, Relationship between coronary artery remodeling and plaque vulnerability, Circulation 105 (2002) 939–943.
[34] P.A. Calvert, D.R. Obaid, M. O'Sullivan, L.M. Shapiro, D. McNab, C.G. Densem, P.M. Schofield, D. Braganza, S.C. Clarke, K.K. Ray, N.E. West, M.R. Bennett, Association between IVUS findings and adverse outcomes in patients with coronary artery disease: the VIVA (VH-IVUS in Vulnerable Atherosclerosis) study, JACC Cardiovasc. Imaging 4 (2011) 894–901.
[35] S. Motoyama, T. Kondo, M. Sarai, A. Sugiura, H. Harigaya, T. Sato, K. Inoue, M. Okumura, J. Ishii, H. Anno, R. Virmani, Y. Ozaki, H. Hishida, J. Narula, Multislice computed tomographic characteristics of coronary lesions in acute coronary syndromes, J. Am. Coll. Cardiol. 50 (2007) 319–326.
[36] D.W. Losordo, K. Rosenfield, J. Kaufman, A. Pieczek, J.M. Isner, Focal compensatory enlargement of human arteries in response to progressive atherosclerosis – in-vivo documentation using intravascular ultrasound, Circulation 89 (1994) 2570–2577.
[37] T. Nishioka, H. Luo, N.L. Eigler, H. Berglund, C.J. Kim, R.J. Siegel, Contribution of inadequate compensatory enlargement to development of human coronary artery stenosis: an in vivo intravascular ultrasound study, J. Am. Coll. Cardiol. 27 (1996) 1571–1576.
[38] G. Pasterkamp, A.H. Schoneveld, A.C. van der Wal, C.C. Haudenschild, R.J. Clarijs, A.E. Becker, B. Hillen, C. Borst, Relation of arterial geometry to luminal narrowing and histologic markers for plaque vulnerability: the remodeling paradox, J. Am. Coll. Cardiol. 32 (1998) 655–662.
[39] Y.J. Hong, M.H. Jeong, Y.H. Choi, J.A. Song, K.H. Lee, D.H. Kim, M.G. Lee, K.H. Park, D.S. Sim, J.H. Kim, Y. Ahn, J.G. Cho, J.C. Park, J.C. Kang, Positive remodeling is associated with vulnerable coronary plaque components regardless of clinical presentation: virtual histology-intravascular ultrasound analysis, J. Am. Coll. Cardiol. 58 (2011). B30–B30.
[40] S.B. Yeon, A. Sabir, M. Clouse, P.O. Martinezclark, D.C. Peters, T.H. Hauser, C.M. Gibson, R. Nezafat, D. Maintz, W.J. Manning, R.M. Botnar, Delayed-enhancement cardiovascular magnetic resonance coronary artery wall imaging – comparison with multislice computed tomography and quantitative coronary angiography, J. Am. Coll. Cardiol. 50 (2007) 441–447.
[41] E. Spuentrup, R.M. Botnar, A.J. Wiethoff, T. Ibrahim, S. Kelle, M. Katoh, M. Ozgun, E. Nagel, J. Vymazal, P.B. Graham, R.W. Gunther, D. Maintz, MR imaging of thrombi using EP-2104R, a fibrin-specific contrast agent: initial results in patients, Eur. Radiol. 18 (2008) 1995–2005.
[42] H. Steen, J.A.C. Lima, S. Chatterjee, A. Kolmakova, F. Gao, E.R. Rodriguez, M. Stuber, High-resolution three-dimensional aortic magnetic resonance angiography and quantitative vessel wall characterization of different atherosclerotic stages in a rabbit model, Investig. Radiol. 42 (2007) 614–621.
[43] K. Croce, P. Libby, Intertwining of thrombosis and inflammation in atherosclerosis, Curr. Opin. Hematol. 14 (2007) 55–61.
[44] G.K. Hansson, Inflammation, atherosclerosis, and coronary artery disease, N. Engl. J. Med. 352 (2005) 1685–1695.
[45] T. Saam, H.R. Underhill, B.C. Chu, N. Takaya, J.M. Cai, N.L. Polissar, C. Yuan, T.S. Hatsukami, Prevalence of American heart association type VI carotid atherosclerotic lesions identified by magnetic resonance imaging for different levels of stenosis as measured by duplex ultrasound, J. Am. Coll. Cardiol. 51 (2008) 1014–1021.
[46] A. Phinikaridou, Y. Qiao, N. Giordano, J.A. Hamilton, Detection of thrombus size and protein content by ex vivo magnetization transfer and diffusion weighted MRI, J. Cardiovasc. Magn. Reson. 14 (2012) 45.

[47] A. Yamashita, Y. Zhao, S. Zhao, Y. Matsuura, C. Sugita, T. Iwakiri, N. Okuyama, K. Ohe, C. Koshimoto, K. Kawai, N. Tamaki, Y. Kuge, Y. Asada, Arterial (18)F-fluorodeoxyglucose uptake reflects balloon catheter-induced thrombus formation and tissue factor expression via nuclear factor-kappaB in rabbit atherosclerotic lesions, Circ. J. 77 (2013) 2626–2635.
[48] A. Yamashita, Y. Asada, A rabbit model of thrombosis on atherosclerotic lesions, J. Biomed. Biotechnol. 2011 (2011) 424929.
[49] F. Liu, D.X. Xu, M.S. Ferguson, B.C. Chu, T. Saam, N. Takaya, T.S. Hatsukami, C. Yuan, W.S. Kerwin, Automated in vivo segmentation of carotid plaque MRI with morphology-enhanced probability maps, Magn. Reson. Med. 55 (2006) 659–668.